

# Failure Prognosis for Permanent Magnet AC Drives Based on Wavelet Analysis

Wesley G. Zanardelli, Elias G. Strangas, and Selin Aviyente

Department of Electrical and Computer Engineering

Michigan State University

East Lansing, MI 48824, USA

e-mail: zanardel@egr.msu.edu

**Abstract**—Prognosis for failure of an electric machine can be achieved through the detection of non-catastrophic faults. As the frequency of these types of faults increases, the working life of the machine is decreased, leading to eventual failure. In this work, two types of stator faults are studied. The methods developed are based on analysis of the Undecimated Discrete Wavelet Transform of the field oriented machine currents. Linear discriminant analysis is used to classify between the fault types.

## I. INTRODUCTION

Reliability of electrical machines and drives is an area of increased attention and research. Diagnosing correctly a failure in an electrical drive can lead to mitigation and continued operation, albeit at reduced power levels.

On the other hand, prior to the fault the drive can show signs of a developing fault, while it is operating normally. Detecting these early signs can lead to appropriate actions before the fault develops.

A wavelet based failure prognosis system was developed for brush DC motors in [1]. The modulus maxima of the Discrete Wavelet Transform (DWT) of the DC current in the machine was analyzed. An algorithm to detect the presence of a fault was based on thresholding of the analysis coefficients. If the detection criterion was met, the coefficients were passed to a classification algorithm. Three classification algorithms were evaluated. The first was based on a decision tree, the second was based on the nearest neighbor rule, and the third was based on linear discriminant analysis. Classification was possible between DC currents in machines with the following faults: increased coil resistance, increased friction, faulty brush springs, rotor misalignment, and damaged commutator face.

A failure prognosis system based on time-frequency analysis was developed for PMAC drives in [2]. Two electrical faults were investigated in this work. The first was a momentary increased resistance in one phase due to a bad connection between the motor and the controller and the second was a turn-to-phase short in the stator windings. Analysis was performed on the bandlimited STFT of the torque producing component of the field oriented stator currents. First, a detection algorithm was based on thresholding of the energy in each FFT sample. If the detection criterion was met, the coefficients were passed to a classification algorithm based on linear discriminant analysis to discriminate between the two faults.

A method to detect turn-turn insulation failures in induction machines is described in [3]. All three line-neutral stator voltages are measured and filtered to remove the fundamental component of the machine excitation voltage. The RMS value of

$v_{sum} = v_{an} + v_{bn} + v_{cn}$  of the filtered components is zero in a balanced machine, however in the case of turn-turn insulation failures, this is not the case. The authors were able to discern between one, two, and three-turn faults. Turn-turn insulation failures lead to turn-ground insulation failures. The technique was implemented offline and is insensitive to changes in the average value of the motor load. One of the main requirements of this technique is the requirement that the machine be star connected with the neutral accessible.

A method based on Finite Element Analysis (FEA) to detect faults in PMAC machines is described in [4]. FEA is used to calculate flux linkages and inductances as functions of rotor position, which are stored in a look-up table and then used in a transient simulation of the motor. This process is repeated for various rotor faults. Spectral analysis is used to determine which harmonics are excited for the various faults. The authors validated the spectral content in the computed currents using experimental results. This technique detects the presence of static and dynamic eccentricities, and flux disturbances originating from defects to the permanent magnets.

The authors determined that the current harmonic components can be analyzed in either the rotor or stationary reference frame. In the case of the static eccentricity, however, analysis in the stationary reference frame was required, since the fault effects in the rotor reference frame were obscured.

The current Park's vector pattern is analyzed for stator voltage unbalance or an open phase in three-phase induction machines in [5]. The Park's vector pattern is plotted in the stationary frame of reference using a two-phase representation of the measured stator currents for one electrical cycle. The plot is analyzed using an Artificial Neural Network (ANN) to check for a stator voltage unbalance or an open phase. The occurrence of either of these faults manifests itself in the deformation of the current Park's vector pattern corresponding to a healthy condition. This deformation leads to an elliptic pattern, whose major axis orientation is associated with the faulty phase. The severity of the deformation helps to distinguish between the two faults, with the open phase fault the most deformed. A mathematical model of the induction motor is not required. This system is implemented offline.

A system to detect mechanical faults in a three-phase induction machine with a gearbox and bearing assemblies is described in [6]. Here, only mechanical vibration is considered in the fault detection algorithm based on input from an accelerometer mounted vertically on top of one of the bearing housings. The wavelet transform using the D4 mother wavelet was applied to the FFT of the accelerometer output. The wavelet trans-

form acted as a preprocessor to an ANN. The ANN was trained to detect faults including the presence of a small 'blip' of 2mm diameter welded onto a gear tooth, a triangle shaped area missing from a gear tooth, and a fractured inner race of the bearing housing. This technique is implemented offline.

Support Vector Machine (SVM) based classification, [7], was used in [8] to classify between faults in induction machines. SVMs are used to map a set of coefficients to a high-dimensional feature space where a set of 'best' separating hyperplanes are constructed. This mapping is based on a set of kernel functions, whose selection is critical. SVMs are binary classifiers, and hence, for multiclass problems, either one-against-all or one-against-one classifiers are developed. In this work, the one-against-one formulation was used requiring  $n(n-1)/2$  classifiers, e.g. for 6 faults (and healthy), 21 classifiers would be required.

Stator line currents, circulating currents between parallel stator branches and forces between the stator and rotor were analyzed. These quantities were computed using FEA and noise was added to them (0 mean, 3% variance of the amplitude of the current). The power spectrum of each signal was used for classification. Faults analyzed included shorted turns, shorted coils, broken rotor bars, broken end rings, rotor eccentricities, and asymmetrical line voltages. Analysis was performed for both 35kW and 1600kW induction motors.

Simulation results showed that classification of faults based on any of the above parameters was possible. Experimental results showed that classification of faults based on stator line currents was possible only when the measurement data was used for both training and testing of the classifier.

In this work, a failure prognosis system is developed to detect signs of developing stator faults in PMAC drives. The faults of interest are non-catastrophic, meaning they allow for continued operation of the motor, but increase the likelihood of failure.

Two types of stator faults are explored, both electrical. The first fault is a momentary increased resistance in one phase due to a bad connection between the motor and the controller. The second fault is a turn-to-phase short, simulating an insulation failure in the stator windings of the motor.

The algorithm is based on analysis of the Undecimated Discrete Wavelet Transform (UDWT) of the torque producing component of the field oriented stator currents. Thresholding on the energy in the UDWT is used to detect a fault in the machine, and linear discriminant analysis is used to classify between the fault types. A collection of observed data is used to train the detection and classification components of the algorithm.

The algorithms developed can be implemented in an online system, using extra processing time in the motor controller.

## II. BACKGROUND

### A. Wavelet Analysis

The Fourier Transform gives the spectrum of a signal. It is best suited for the analysis of stationary signals, or signals whose spectrum remains constant. The FFT is used to determine the spectrum of discrete-time signals. Tiling in the time-frequency plane for the FFT in Fig. 1 shows that the spectrum of the signal is divided into several frequency bands, however

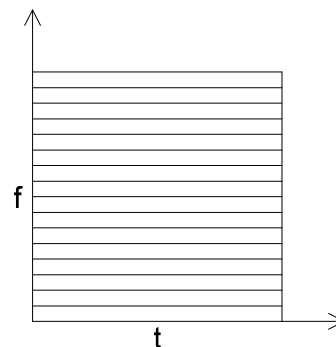


Fig. 1. FFT Tiling

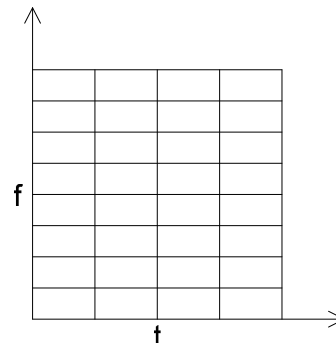


Fig. 2. STFT Tiling

no information is present on the time axis. The faults studied in this work manifest themselves as short transients superimposed on the stator currents. Analysis of these short transients, however, requires information in both frequency and time. The inability to provide time localization of a signal is a fundamental limitation of the FFT.

The STFT [9] is an extension of the FFT, allowing for the analysis of non-stationary signals. Here, the signal is divided into small time sections, and each is analyzed using the FFT. The results for of the STFT are intuitive and easy to correlate with the original signal. Tiling for the STFT in Fig. 2 shows how the spectrum of a signal changes with time. The tiling for the STFT is uniform in both time and frequency. In the implementation of the STFT, a design tradeoff must be made between time and frequency resolution. This is due to the uncertainty principle, which limits the lower bound on the time-bandwidth product (1).

$$TB \geq \frac{1}{2} \quad (1)$$

A block diagram for the STFT algorithm is shown in Fig. 3, where  $nfft$  is the length of the DFT,  $noverlap$  is the number of samples the two frames overlap, and  $window$  is a weighting vector applied to the FFT input. The spectrogram is a plot of the magnitude square of the STFT. It is similar to the tiling shown in Fig. 2, with color shading denoting the energy in each tile.

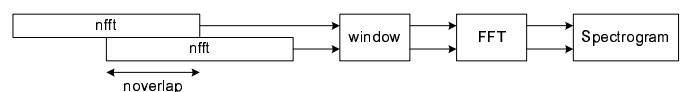


Fig. 3. STFT Block Diagram

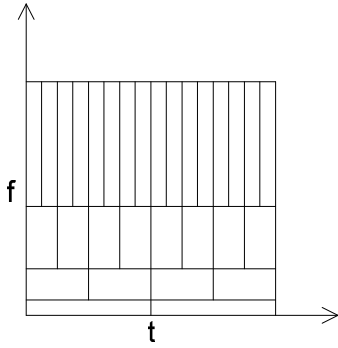


Fig. 4. DWT Tiling

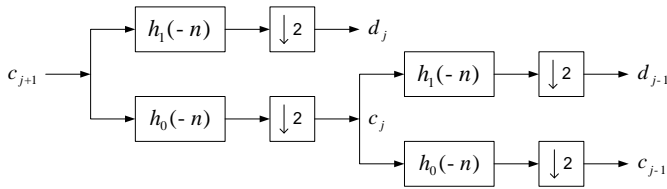


Fig. 5. Two-Stage DWT Filter Bank Analysis Tree

Wavelet analysis [10] is also suitable for non-stationary signals. The DWT has greater flexibility than the STFT. Different basis functions, or mother wavelets, may be used in Wavelet analysis while the basis function for Fourier analysis is always the sinusoid. Unlike sinusoids, wavelets have finite energy concentrated around a point in time. One can choose, or design a wavelet to achieve the best results for a specific application.

Tiling for the DWT is shown in Fig. 4. The tiling for the DWT is variable, allowing for both good time resolution of high frequency components, and good frequency resolution of low frequency components in the same analysis.

A block diagram for the DWT algorithm using filter banks is shown in Fig. 5, where  $c$  and  $d$  are the scaling and wavelet function coefficients, and  $h_1$  and  $h_0$  are the decomposition highpass and lowpass filters.

One of the drawbacks of the DWT is that it is not a shift-invariant transformation. This makes pattern recognition problems based on the DWT more difficult, since the DWT coefficients resulting from decomposition of a signal and a shifted version of the signal can be very different. Only in special cases, where the signal is shifted by specific powers of 2 will the outputs be shifted versions of one another.

The UDWT adds the property of shift-invariance to the DWT. Here, the downsampling step is omitted from the DWT algorithm, and zeros are inserted between the filter coefficients at each successive scale, as shown in Fig. 6. This is known as the “Algorithme à Trous” [11, 12]. While circular convolution is used in [11], linear convolution is used here, since the signals are not periodic. The coefficients at each end of the convolution where the filter and the signal are not completely overlapping, known as end effects, are replaced by zeros. As these zeros propagate through each scale of the UDWT, the number of end effect coefficients increases. The fact that the length of the wavelet filters increase at each scale also contributes to additional end effects.

An example to show the shift-invariant property of the

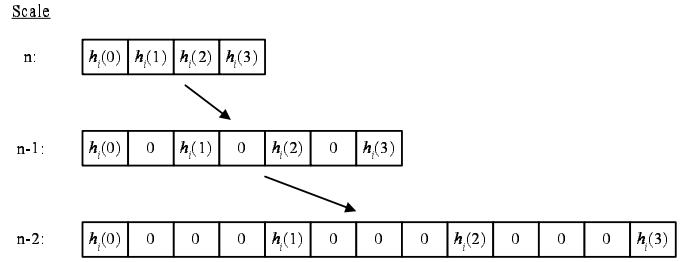


Fig. 6. UDWT Filters Modified by the “Algorithme à Trous”

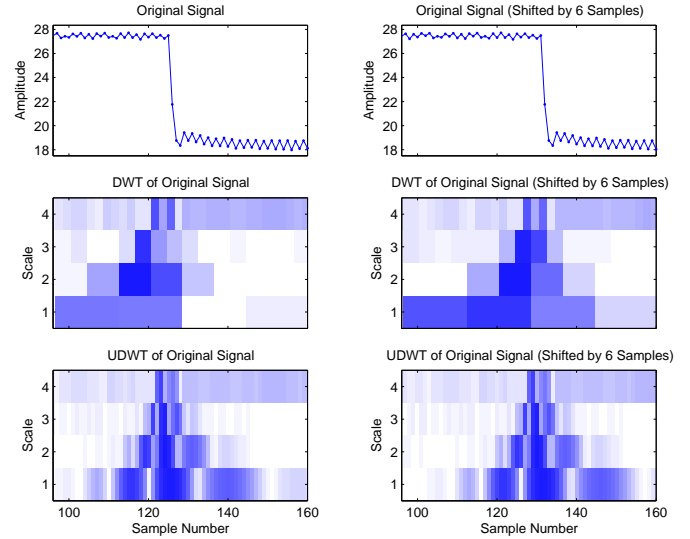


Fig. 7. Example of Shift-Invariance of the UDWT

UDWT is in Fig. 7. Here, the DWT and UDWT of a signal and the same signal shifted by 6 samples are compared. The first row shows the non-shifted and shifted signals. The second and third rows show the DWT and UDWT of these signals. The value of the wavelet coefficients is denoted by shading, with the darkest coefficients having the highest amplitude. In the case of the DWT, it can be seen that the distribution of energy in the wavelet coefficients is different for the non-shifted and shifted signals. For the UDWT, the distribution of energy is consistent for both signals, with the output coefficients shifted by the same number of samples as the input signal.

In this work, analysis is based on the UDWT, as it offers the greatest flexibility and is shift-invariant. Results based on each analysis technique will be compared.

## B. Pattern Recognition

Once the UDWT coefficients have been determined, the presence of a fault is detected based on thresholding of the energy in the coefficients. The next step is to vectorize the coefficients allowing for the use of discriminant analysis for classification. The vectorization process combines columns of the UDWT into a vector. Vectorization of the data begins when the criterion for detection is met. An example of vectorization using  $N$  time samples is shown in Fig. 8.

In the implementation of discriminant functions, no prior knowledge of a probability distribution among the sample points is assumed. The space is divided into  $K$  regions, each

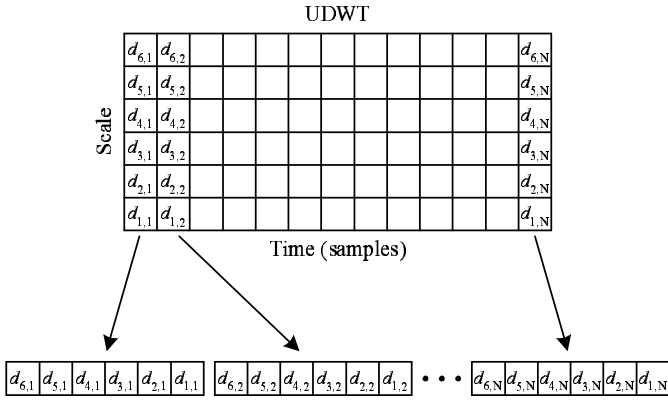


Fig. 8. Vectorization of  $N$  Samples of the UDWT

having its own weighting coefficients. In this work, we use linear discriminant functions (2) [13],

$$D_k(\mathbf{x}) = x_1\alpha_{1k} + x_2\alpha_{2k} + \dots + x_N\alpha_{Nk} + \alpha_{N+1,k} \quad (2)$$

$$k = 1, 2, \dots, K$$

where  $x$  is the  $N$ -dimensional sample vector and  $\alpha$  are the normalized weighting coefficients for the  $k$ -th class. A sample vector belongs to a particular class if its discriminant function is greater for that class than for any other class, i.e.,  $\mathbf{x}_i$  belongs to class  $C_j$  if

$$D_j(\mathbf{x}) > D_k(\mathbf{x}) \quad \text{for every } k \neq j.$$

The weighting coefficients are adjusted from their initial guess through a training procedure using sample vectors which the proper classification is known. The algorithm for this procedure makes adjustments to the weighting coefficients until each sample vector is correctly classified.

Young and Calvert [13] show that this training algorithm will converge in a finite number of steps. When a sample vector is correctly classified, no adjustment to the weighting coefficients is made. When a sample vectors is incorrectly classified, or

$$D_j(\mathbf{x}) \leq D_l(\mathbf{x}),$$

where

$$D_l(\mathbf{x}) = \max_{l \neq j} [D_1(\mathbf{x}), \dots, D_K(\mathbf{x})],$$

adjustments are made to  $\alpha_j$  (3) and  $\alpha_l$  (4) only,

$$\alpha_j(i+1) = \alpha_j(i) + a\mathbf{x}_i \quad (3)$$

$$\alpha_l(i+1) = \alpha_l(i) - a\mathbf{x}_i, \quad (4)$$

where  $a$  is a gain constant.

### III. FAULTS EXPLORED

The test machine used in this analysis is a six-pole surface mounted PMAC machine for an automotive application. The machine is operated using constant torque-angle control [14] in a vector drive with the torque angle set to  $\pi/2$ . This mode of operation minimizes losses in the machine, and is suitable for operating speeds up to the base speed. Conditions for the tests in this work follow: The torque-producing component of the stator current command  $i_{qs}^* = 0.3pu$ , and the flux-weakening component  $i_{ds}^* = 0$ ; the speed is controlled by the dynamometer and is set to 1/10 the no-load speed.

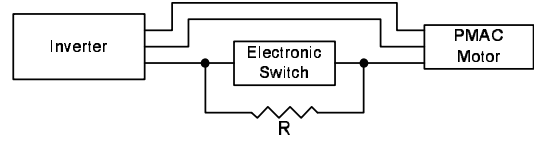


Fig. 9. Series Resistance Fault

#### A. Series Resistance

The first fault explored in this work is an intermittent increased contact resistance between the motor and the controller. An experimental setup was designed to simulate this. The fault is achieved by adding the parallel combination of a normally closed switch and a resistance in series with one of the motor phases. A circuit diagram is shown in Fig. 9.

The fault is initiated by opening the switch for a short time interval causing current to flow through the resistance. The switch is described in detail in Section V.

The value of the series resistance is approximately ten times the value of the stator resistance,  $R_s$ . The fault is initiated as the phase current command rises to 95% of its peak amplitude. Tests with fault durations of 5ms and 10ms have been performed to investigate invariance of the results with respect to this parameter.

#### B. Turn-To-Phase Short

The second fault explored in this work is an insulation failure in the stator windings of the motor. The machine used in this experiment has multiple parallel windings per phase, each with several coils in series. Stranded wire is used. To simulate this fault in the experimental setup, at one point in a single strand of one of the windings, the insulation was removed, and a normally open switch was added between this point and the corresponding phase terminal of the motor. The fault was initiated by momentarily closing the switch, causing current to be split between the intended path and the switch.

The fault is initiated as the phase current command rises to 95% of its peak amplitude. Tests with fault durations of 5ms and 10ms have been performed to investigate invariance of the results with respect to this parameter.

## IV. ANALYSIS METHODS

In this work, the detection and classification of the faults described in Section III are based on analysis of the stator currents of the machine. Rather than analyzing the three phase stator currents independently of each other, the field oriented currents  $i_{qs}$  and  $i_{ds}$  are used. This has the advantage that the fundamental electrical frequency is not present. Consequently, rotor speed has little effect on the spectrum of these currents, allowing for invariance in the algorithm to rotor speed. Together,  $i_{qs}$  and  $i_{ds}$  are a complete representation of the stator currents, however, it has been determined experimentally that through analysis of  $i_{qs}$  only, accurate fault detection and classification can be achieved.

The controller time constant is longer than the transients that occur at the edges of the faults explored in this work. While the selection of gains in the controller has a significant effect on the

currents during and after a fault occurs, controller correction of the currents has a negligible effect on the transients at the inception and the clearing of a fault.

The input to the detection and classification algorithm is a subset of the UDWT of the measured q-axis current,  $i_{qs}$ . For this analysis, the Daubechies D4 mother wavelet was used and decomposition was performed to 6 levels.

The algorithm has two parts; a detection phase and a classification phase. The detection phase of the algorithm is based on thresholding of the weighted energy of the UDWT. The weighted energy is defined in (5).

$$E(x) = \sum_{n=1}^6 d_{n,x}^2 \cdot 2^{n-1} \quad (5)$$

The weighting gives more emphasis to the high frequency information in the current. The threshold on the weighted energy was set to be 40% greater than the largest which was observed in all samples from the healthy machine data. If the weighted energy in new test data exceeds this threshold, a fault is considered to exist. The sample index which will be used for classification is the index of the local maxima of the weighted energy of the 64 points beginning from where the threshold was exceeded.

The classification phase was based on linear discriminant analysis and is implemented when the criterion for detection is met. Two classes were created for each fault; one corresponding to the inception, and the other to the clearing of the fault. The advantage of two separate classes for each fault is invariance to the duration of the fault. Additionally, a postprocessing algorithm to verify that subsequent classification of the beginning and end of the same fault type would further confirm existence of the fault. To train the algorithm, thereby determining the weighting coefficients, data were used from 16 experiments corresponding to both faults with  $5ms$  and  $10ms$  switch durations. The data used were the 64 samples in the UDWT, beginning 8 samples prior to the event.

Following the training of the weighting coefficients, data that had not been used in the training algorithm were tested. Two data sets from each of the following operating conditions were tested: Healthy,  $5ms$  series resistance,  $10ms$  series resistance,  $5ms$  turn-to-phase short, and  $10ms$  turn-to-phase short.

FEA results using Flux2D were considered for use in training the detection and classification algorithms, however the spectrum of the preliminary FEA results was significantly different than that of the experimental results. The use of FEA would allow for increased flexibility, giving more training samples, for the faults explored. One fault detection approach based on results from FEA was described in [4]. Improvements in the FEA model are expected to decrease the difference between the results, however, there are still phenomena which will be difficult to model, e.g. the switching in a PWM inverter, requiring very small time steps, as well as the inclusion of required parasitic capacitances.

## V. EXPERIMENTAL SETUP

A block diagram for the experimental setup is shown in Fig. 10. A PC running RT-Linux was used as the controller for this

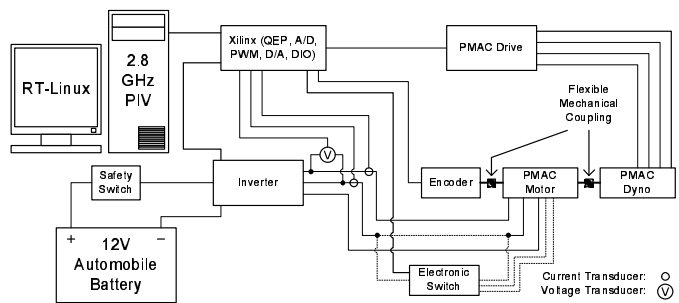


Fig. 10. Experimental Setup Block Diagram

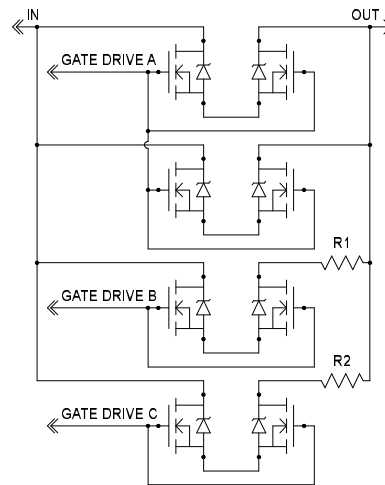


Fig. 11. Electronic Switch

project. The PC is superior to a DSP in terms of cost, CPU power, and memory capacity. A fundamental limitation of the PC, however, is the limited I/O capability. To remedy this, a custom Xilinx FPGA based I/O board was developed. The I/O board inputs include 12 analog channels and a counter for a quadrature encoder. Outputs include 12 PWM/digital and 4 analog channels. Communication between the I/O board and the PC is via the parallel port.

Two phase currents were measured using current transducers with rated accuracy of 0.45% and bandwidth of  $0 - 200kHz$ . A single line-line voltage for use in the initial position calibration was measured as well.

A quadrature encoder with 1024 counts per revolution (4096 for quadrature) and an index pulse was used to measure the rotor position.

A bi-directionally conducting electronic switch was designed to initiate faults in the stator. This switch, as shown by the dotted lines in Fig. 10, can be configured to initiate either the series resistance fault or the turn-to-phase short. A circuit diagram for the electronic switch is shown in Fig. 11.  $R_{DS(ON)}$  for each MOSFET is approximately one-third the resistance of a single turn of a single strand in one of the stator coils. The switch can be controlled using digital outputs or PWM to create a resistance profile.

## VI. RESULTS

The results from two typical test cases are shown in Fig. 12. On the left side of Fig. 12 are results from the series resistance

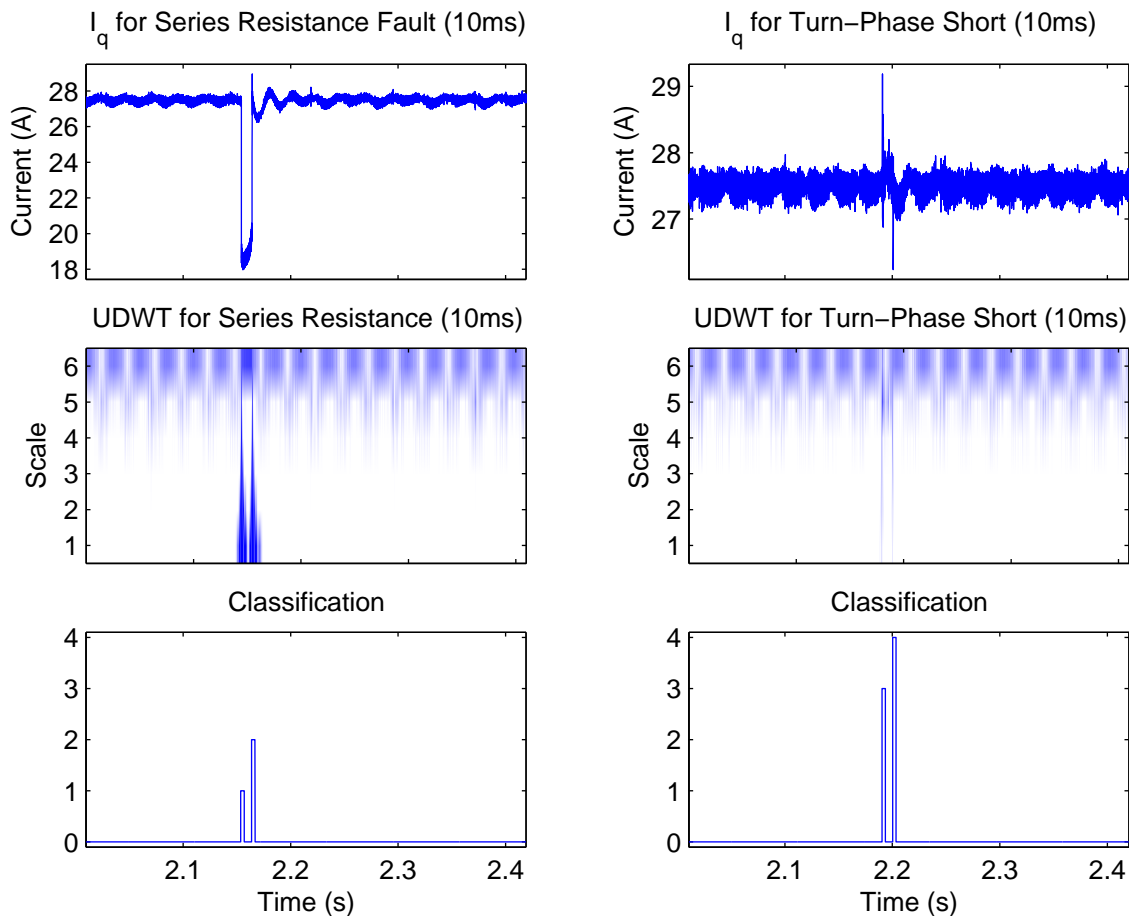


Fig. 12. Typical Results

fault, and on the right side are results from the turn-to-phase short. The first row shows the q-axis, or torque producing component, of the current. The second row shows the UDWT of the above currents. The third row shows the output of the detection and classification algorithm, with 0=Healthy, 1=Beginning of Series Resistance Fault, 2=End of Series Resistance Fault, 3=Beginning of Turn-to-Phase Short, and 4=End of Turn-to-Phase Short. The results presented are based on new data not used in the training set.

In Fig. 12, it can be seen that the amplitude of the UDWT coefficients is increased at the points of inception and clearing of the faults. The increased energy at these points meets the criterion for detection, and the classification algorithm operates on the UDWT coefficients corresponding to 3.2ms of data at these points. The results shown indicate correct classification of the inception and clearing of both faults explored in this work.

The ten tests described in Section IV resulted in no false positives and one false negative. In the two healthy cases, no fault events were detected. In the four cases with the series resistance fault, all fault inception and clearing events were identified correctly. In the four cases with the turn-to-phase short, three of the four fault inception events were identified correctly, and the fourth did not meet the criterion for detection; all four fault clearing events were identified correctly.

## VII. CONCLUSIONS

An algorithm capable of giving a prognosis for failure of a PMAC drive has been developed. It is based on the detection and classification of small transients in the stator currents corresponding to non-catastrophic faults. Early detection of these faults can give indication when maintenance or mitigation is required, minimizing the likelihood of system failure.

The UDWT, used in this work, is shift-invariant and offers good time resolution of high frequency components and good time and frequency resolution of low frequency components in the same analysis. The UDWT allows for increased flexibility and resolution when compared to the more traditional FFT and STFT, and overcomes the drawbacks of the DWT.

The categorization algorithm uses a linear discriminant function and is trained using a set of operating conditions which include healthy drives and samples of faulted drives. An exhaustive set of such conditions is necessary to develop a robust algorithm.

Although the algorithms in this work were used offline, they can be added to an existing motor controller enabling them to run close to real-time. The vector currents are typically calculated as part of the control. Minimal, if any, additional CPU speed and memory capacity would be required ensuring a low-cost system. The training phase of the algorithms would remain offline.

## ACKNOWLEDGMENT

The authors thank Tomy Sebastian, Sayeed Mir, Mohammad Islam, and Avoki Omekanda from Delphi Corporation for their continued guidance and support in this research project.

## REFERENCES

- [1] W. G. Zanardelli, E. G. Strangas, H. K. Khalil, and J. M. Miller, "Wavelet-based methods for the prognosis of mechanical and electrical failures in electric motors," *Mechanical Systems and Signal Processing*, pp. 411–426, Mar. 2005.
- [2] W. G. Zanardelli and E. G. Strangas, "Failure prognosis for permanent magnet ac machines based on time-frequency analysis," in *International Conference on Electrical Machines*, Sep. 2004.
- [3] A. Cash, T. G. Habetler, and G. B. Kliman, "Insulation failure prediction in ac machines using line-neutral voltages," *IEEE Transactions on Industry Applications*, vol. 34, pp. 1234–1239, Nov.–Dec. 1998.
- [4] W. le Roux, R. G. Harley, and T. G. Habetler, "Rotor fault analysis of a permanent magnet synchronous machine," in *International Conference on Electrical Machines*, 2002.
- [5] H. Nejari and M. E. Benbouzid, "Monitoring and diagnosis of induction motors electrical faults using a current park's vector pattern learning approach," *IEEE Transactions on Industry Applications*, vol. 36, pp. 730–735, May–Jun. 2000.
- [6] B. A. Paya, I. I. Esat, and M. N. M. Badi, "Artificial neural network based fault diagnostics of rotating machinery using wavelet transforms as a pre-processor," *Mechanical Systems and Signal Processing*, vol. 11, pp. 751–765, Sep. 1997.
- [7] A. R. Webb, *Statistical Pattern Recognition*. John Wiley & Sons, 2nd ed., 2002.
- [8] S. Pöyhönen, M. Negrea, P. Jover, A. Arkkio, and H. Hyötyniemi, "Numerical magnetic field analysis and signal processing for fault diagnostics of electrical machines," in *International Conference on Electrical Machines*, Aug. 2002.
- [9] L. Cohen, *Time-Frequency Analysis*. Prentice Hall, 1995.
- [10] C. S. Burrus, R. A. Gopinath, and H. Guo, *Introduction to Wavelets and Wavelet Transforms, A Primer*. Prentice Hall, 1998.
- [11] S. Mallat, *A Wavelet Tour of Signal Processing*. Academic Press, 2nd ed., 1999.
- [12] P. Dutilleul, "An implementation of the "algorithme à trous" to compute the wavelet transform," in *Wavelets: Time-Frequency Methods and Phase Space, Proceedings of the International Conference*, Springer-Verlag, 1987.
- [13] T. Y. Young and T. W. Calvert, *Classification, Estimation and Pattern Recognition*. American Elsevier Publishing Co., Inc., 1974.
- [14] R. Krishnan, *Electric Motor Drives: Modeling, Analysis, and Control*. Prentice Hall, 2001.